

POLE MASSES OF NEUTRINOS IN THE GRIMUS–NEUFELD MODEL*

VYTAUTAS DŪDĖNAS, THOMAS GAJDOSIK, DARIUS JURČIUKONIS

Institute of Theoretical Physics and Astronomy
Faculty of Physics, Vilnius University

(Received November 5, 2019)

We present a comparison of pole mass calculations in the Grimus–Neufeld model. Pole masses are calculated in three different ways: using the approximation of Grimus and Lavoura, using a one-loop approximation and using FlexibleSUSY, an automated spectrum generator. We present the differences between these calculations and compare them numerically in the parameter region that could potentially reproduce the measured neutrino mass squared differences.

DOI:10.5506/APhysPolB.50.1737

1. Introduction

Neutrino masses are not zero. This has been already known for about 30 years, yet, not much is known about their nature. A popular mechanism that naturally explains the smallness of neutrino masses is the seesaw mechanism [1]. However, as it usually gives the masses at tree level in a simple enough way, the phenomenological one-loop studies on the interplay of the neutrino sector with some other beyond the Standard Model (BSM) sectors are rather rare. One of the models that can have some restrictions on the neutrino sector relating it to the scalar sector is the Grimus–Neufeld model (GNM) [2]. It is a two-Higgs doublet model (2HDM) extended with a single heavy Majorana neutrino. This set-up gives two non-vanishing light neutrino masses at one-loop level, which is already enough to explain the two experimentally measured mass squared differences. The non-trivial feature of this model is that there is a subtle interplay between the radiative mass generation and the seesaw mechanism. This interplay is used in the Grimus–Lavoura (GL) approximation [3, 4], realizing that the seesaw suppressed tree-level mass can numerically be of the same order as loop corrections. We show that this approximation can be understood as a perturbation

* Presented at the XLIII International Conference of Theoretical Physics “Matter to the Deepest”, Chorzów, Poland, September 1–6, 2019.

series in couplings rather than in loops. This elucidates an unusual feature of the seesaw mechanism: the coupling expansion is different from the loop expansion. The benefit of the GL approach is that the resulting expressions for pole masses are gauge-invariant and finite without the need of any subtraction scheme.

On the other hand, in the full one-loop calculation of neutrino masses, one needs to determine mass and field renormalization constants. We will calculate the one-loop pole masses in the $\overline{\text{MS}}$ scheme and compare them to the GL approximation. To get an idea what are really the differences between the first order pole masses in loop expansion *versus* the first order pole masses in Yukawa coupling expansion, we systematically ignore the higher order terms. This means that the off-diagonal one-loop contributions to the mass matrix do not enter the pole mass expressions, as they come as $O((1 \text{ loop})^2) = O(2 \text{ loop})$.

Yet another way to calculate masses of neutrinos in the GNM is to implement the model into the automated spectrum generator FlexibleSUSY [5, 6] (FS). FS also uses $\overline{\text{MS}}$ to calculate neutrino masses at one loop. However, it does not neglect the mentioned off-diagonal terms, as it evaluates all the one-loop two-point functions numerically in a full 4×4 matrix and solves the equation for the poles of neutrinos directly. The difference between our pole mass calculation in $\overline{\text{MS}}$ should formally be of higher order in the perturbation series. As we will see in the numerical comparisons, this difference is, in fact, significant and FS calculations are actually closer to the GL approximation.

In Section 2, we shortly present the essential parts of the model that will be needed to understand the calculations. In Section 3, we introduce and explain the differences between the GL approximation, the one-loop approximation, and the FS calculation of pole masses of neutrinos in the GNM. In Section 4, we illustrate the differences between the calculations by a numerical comparison.

2. The model for the masses

A detailed presentation of the model can be found in [2, 7–9]. Here, we will present only the essential parts for our calculations from the scalar and the Yukawa sector of the model.

2.1. Scalar sector

The scalar sector of the GNM is a general 2HDM. We will label the two Higgs doublets as H_1 and H_2 . We choose the Higgs basis, which means that

$$\langle H_1 \rangle = \frac{1}{\sqrt{2}}v, \quad \langle H_2 \rangle = 0, \quad (1)$$

where the value v coincides with the value of the vacuum expectation value (VEV) of the Higgs of the SM ($v = 246.22$ GeV in our analysis). Hence, we can call H_1 to be an SM-like Higgs doublet and H_2 the second Higgs doublet. Three of the degrees of freedom in H_1 are Goldstone bosons. We work in general R_ξ gauge when checking the gauge independence of the GL approximation and in $\xi = 1$ gauge for calculations in the full one-loop approximation. FS calculations are done in $\xi = 1$ gauge. For simplicity, we work in the CP symmetric 2HDM potential, which means that CP-odd and CP-even scalar components of the doublets do not mix at tree level. A review of the various parametrizations and the analysis of the 2HDM can be found in [10].

2.2. Yukawa sector and neutrino masses

We start from the flavour basis, where the three light neutrinos are labeled by their charged weak partners. Then, including one singlet Weyl spinor N with a Majorana mass M , the Yukawa Lagrangian part that leads to neutrino masses is written as

$$\mathcal{L}_{\text{Yuk}} = -Y_{\nu_i}^1 \ell_i H_1 N - Y_{\nu_i}^2 \ell_i H_2 N + \text{H.c.}, \quad i = e, \mu, \tau, \quad (2)$$

where i is the flavour index and ℓ is the lepton doublet in terms of Weyl spinors. We can always find the unitary transformation U on the light SM-like neutrino fields in the lepton doublet ℓ that will lead to the following form of Yukawa couplings [2]:

$$U\nu = \nu', \quad Y_\nu^1 U = (0, 0, y), \quad Y_\nu^2 U = (0, d, d'). \quad (3)$$

After the electroweak symmetry breaking takes place, ν_3 gets a Majorana mass from the effective dimension 5 operator after the N field is integrated out

$$m_3 \approx \frac{y^2 v^2}{2M} \quad (4)$$

in the limit, where M is large. This is the usual type I seesaw mechanism [1, 11]. With the parametrization of Eq. (3), the seesaw mechanism in the GNM can be illustrated by the Feynman diagram shown in Fig. 1(a)¹. From the basis choices, Eq. (3) and Eq. (1), we can see that this is the only seesaw-generated mass in the model, since ν_3 is the only neutrino directly interacting with the SM-like Higgs doublet. This means that the other two light neutrinos stay massless at tree level.

¹ See the Weyl spinor notation in *e.g.*, [12] for Feynman rules with Weyl spinors.

At one-loop level, the second Higgs doublet allows for a similar diagram for neutrino ν_2 , shown in Fig. 1 (b). As one can see, the principle difference of Fig. 1 (b) from Fig. 1 (a) is that the scalar propagator line is closed and forms a loop, instead of the two lines ending in the Higgs VEV. Hence, the diagram in Fig. 1 (b) is responsible for radiative mass generation for ν_2 , which is also suppressed by $\sim \frac{1}{M}$ similarly to the tree-level seesaw mechanism.

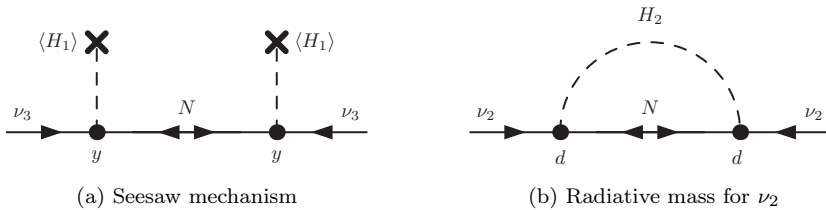


Fig. 1. Seesaw and radiative mass generation in Weyl spinor notation [12]. The arrow shows chirality propagation.

From now on, we write μ to denote loop-level masses and m to denote tree-level masses. The basis choice of Eq. (3) lets us identify the four distinct neutrino one-loop mass states ν_i with the heavy mass $\mu_4 \approx m_4$, the small seesaw mass μ_3 , the radiative mass μ_2 , and zero mass. Hence, the matrix U is actually an approximate PMNS (Pontecorvo–Maki–Nakagawa–Sakata) matrix, U_{PMNS} , which relates the mass eigenstates to the flavor states of neutrinos. As the PMNS matrix is given by the experiment, the only parameters that are still free in the neutrino Yukawa sector are y , d and d' . The further step is to relate these parameters to the measured neutrino mass differences, for which we need to calculate pole masses of neutrinos.

3. Pole mass calculation

We define the two-point Green's functions for neutrinos according to their Lorentz structure as in Fig. 2, where Γ and Σ are scalar functions; the spinoric indices are factored out. The arrow shows the chirality propagation of Weyl spinors, hence Γ stands for a chirality flipping (mass-like) two-point function, and Σ for a chirality preserving one (usually noted as field renormalization part). As neutrinos in the GNM are Majorana particles, we do not have two independent contributions for field renormalization, hence there is only one Σ with no label for chirality. The Σ matrix is Hermitian for stable particles. In the calculations presented in the conference [13], we assumed that Γ is also Hermitian. However, that is not true in general. As a result, the pole masses for GL approximation changed, as shown here (*i.e.* in Eq. (12)). The one-loop expressions, Eq. (9), stay the same. This correction for the GL approximation has an impact in those parameter points in

which the singular values of Γ do not coincide with the eigenvalues squared. A better agreement between the GL approximation and FS is seen in the corrected plots, shown in Fig. 3 and Fig. 4, than in the ones presented in the conference.

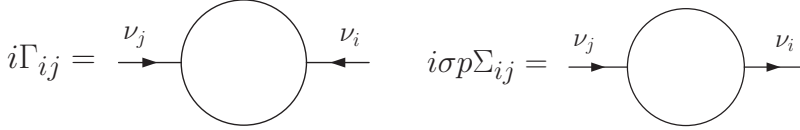


Fig. 2. Chirality flipping and chirality preserving two-point functions for neutrinos.

We indicate the Hermitian conjugate by $\bar{\Gamma}$, where the bar means that we conjugate only couplings that appear in front of the loop integrals, but we do not conjugate the loop integrals themselves. However, for diagonal terms, we can always achieve $\Gamma_{ii} = \bar{\Gamma}_{ii}$ by adjusting the Majorana phases.

Having Γ and Σ , we can get pole masses from solving the equation for μ [14]

$$\det(\mu^2 \Sigma - \bar{\Gamma} \Sigma^{-1} \Gamma) = 0. \quad (5)$$

Since we usually do not know the full expression of the two-point functions, we expand them in a perturbation series, hence we solve Eq. (5) perturbatively

$$\mu = \sum_n \epsilon^n \mu^{[n]}, \quad \Sigma = \sum_n \epsilon^n \Sigma^{[n]}, \quad \Gamma = \sum_n \epsilon^n \Gamma^{[n]}, \quad (6)$$

where ϵ is the order parameter of the perturbation series. Usually, ϵ is identified with the loop counting parameter, but this is not the only identification possible. Further, we will consider two cases: where the power of ϵ counts the number of loops and where it counts the number of Yukawa couplings.

3.1. One-loop approximation

In the loop expansion of the two-point functions, the zeroth order (*i.e.* tree level) 4×4 mass matrix for the neutrinos in the GNM is

$$\Gamma^{[0]} = - \begin{pmatrix} 0 & 0 & 0 & 0 \\ 0 & 0 & 0 & 0 \\ 0 & 0 & m_3 & 0 \\ 0 & 0 & 0 & m_4 \end{pmatrix} \quad \text{with} \quad m_3 \approx \frac{y^2 v^2}{2M}, \quad m_4 \approx M. \quad (7)$$

$\Sigma^{[0]}$ is the identity matrix. We generate the loop functions using FeynArts [15] and FormCalc [16, 17]. $\Sigma^{[1]}$ has contributions in all of its 4×4

matrix elements at one loop. However, due to the basis choice of Eq. (3), some elements in $\Gamma^{[1]}$ are zero, giving the structure

$$\Gamma^{[1]} = \begin{pmatrix} 0 & 0 & * & * \\ 0 & * & * & * \\ * & * & * & * \\ * & * & * & * \end{pmatrix}. \quad (8)$$

With this structure in mind, we write Eq. (6) to the order of $n = 1$, insert into Eq. (5) and solve for the first order in ϵ , evaluating functions at each zeroth order solution. The result for the four one-loop pole masses is

$$\begin{aligned} \mu_1 &= 0, & \mu_3 &= m_3 - \frac{1}{2} \left(\Gamma_{33}^{[1]}(m_3^2) + \bar{\Gamma}_{33}^{[1]}(m_3^2) \right) - m_3 \Sigma_{33}^{[1]}(m_3^2), \\ \mu_2 &= -\Gamma_{22}^{[1]}(0), & \mu_4 &= m_4 - \frac{1}{2} \left(\Gamma_{44}^{[1]}(m_4^2) + \bar{\Gamma}_{44}^{[1]}(m_4^2) \right) - m_4 \Sigma_{44}^{[1]}(m_4^2). \end{aligned} \quad (9)$$

This solution is written in the form which is independent of the renormalization scheme, *i.e.* counterterms appear in the loop functions $\Gamma^{[1]}$ and $\Sigma^{[1]}$ that arise from the redefinition of tree level $\Gamma^{[0]}$ and $\Sigma^{[0]}$. This basically means that we need to define a scheme for absorbing the ultraviolet (UV) divergences that arise in $\Gamma^{[1]}$ and $\Sigma^{[1]}$. For example, the OS scheme would lead to $\mu_3 = m_3$ and $\mu_4 = m_4$. However, in this specific case, the one-loop μ_1 and μ_2 are finite and gauge-invariant without any subtraction scheme. This is obvious for μ_1 , but for μ_2 , the cancellation of divergences in $\Gamma_{22}^{[1]}(0)$ might not sound so obvious. The fact that μ_2 is gauge-invariant and finite comes directly from the fact that the zeroth order solution for μ_2 is 0. This means that, assuming multiplicative renormalization, we do not have any counterterm to absorb potential UV divergences or counteract gauge dependencies at one loop. Thus, the one-loop expression must be gauge-independent and finite by itself. This nice interplay between the renormalization and the perturbation series expansion will be put even further in the Grimus–Lavoura approximation.

Looking at the expressions of Eq. (9), one can see that the off-diagonal terms of the two-point functions are absent in these expressions: they are formally of a higher loop order. Consider, however, that we choose the $\overline{\text{MS}}$ scheme to absorb the divergences of all the two-point functions, and try to get the pole masses numerically. We then can straightforwardly solve Eq. (5) with the full, numerical one-loop 4×4 matrices. The differences in the pole masses should, in principle, be of a higher order in the perturbation series.

3.2. Grimus–Lavoura approximation

We are interested only in the three light neutrino states, *i.e.* the states that are already known to exist. We would like to have a gauge-invariant

and finite relation between the Yukawa parameters Eq. (3) and pole masses of light neutrinos. Then, inspired by the example of radiative neutrino mass generation, we can try to define our perturbation series in such a way, that all of the neutrinos are massless at zeroth order. The next order should then give the finite and gauge-invariant expressions for neutrino masses. How can we do that?

By looking at the two diagrams in Fig. 1, we see that the seesaw diagram, in fact, has the same number of Yukawa couplings as the loop diagram: the coupling expansion is different than the loop expansion. This means that we can try to expand in couplings. To achieve that, we write all the fermion masses in terms of couplings and the VEV of the Higgs. Then, to expand to the second power in couplings, we observe that it is enough to consider one loop, as higher loops will include only higher powers in couplings. Hence, we can use the same tree and one-loop functions and expand them in powers of Yukawa couplings. The tree level and the one-loop level has to be treated together, since we do not want to have a loop ordering, but a coupling ordering instead. With this procedure, we recover the same expressions for neutrino mass matrix entries as in [3]. The structure of the 4×4 mass matrices is now different from the ones shown in Eq. (7) and Eq. (8)

$$\Gamma^{[0]} = - \begin{pmatrix} 0 & 0 & 0 & 0 \\ 0 & 0 & 0 & 0 \\ 0 & 0 & 0 & 0 \\ 0 & 0 & 0 & m_4 \end{pmatrix}, \quad \Gamma^{[1]} = \begin{pmatrix} 0 & 0 & 0 & * \\ 0 & * & * & * \\ 0 & * & m_3 + * & * \\ * & * & * & * \end{pmatrix}. \quad (10)$$

Inserting this $\Gamma^{[0]} + \epsilon \Gamma^{[1]}$ into Eq. (5) and collecting terms near the same power of ϵ will give solutions for μ_2 and μ_3 , satisfying

$$\mu_2^2 \mu_3^2 = [\Gamma_{23}^2 - \Gamma_{22} (\Gamma_{33} - m_3)] [\bar{\Gamma}_{23}^2 - \bar{\Gamma}_{22} (\bar{\Gamma}_{33} - m_3)], \quad (11)$$

$$\mu_2^2 + \mu_3^2 = \Gamma_{22} \bar{\Gamma}_{22} + 2 \Gamma_{23} \bar{\Gamma}_{23} + (m_3 - \Gamma_{22}) (m_3 - \bar{\Gamma}_{33}). \quad (12)$$

Both of these expressions are finite and gauge-invariant without any UV subtraction. Moreover, it can be shown [8] that the expression of Eq. (11) does not depend on d' from Eq. (3), but only on y , d and the scalar potential parameters. The expression in Eq. (12) depends on all the Yukawa parameters from Eq. (3) and the scalar potential parameters. Note that the off-diagonal terms are important already at the first order in the expansion, in contrast to the Eq. (9). Note also that $\Gamma^{[1]}$ in the GL approximation is different from $\Gamma^{[1]}$ in the loop expansion, as the perturbation expansion parameter is different.

3.3. FlexibleSUSY mass calculations

One of our goals is to explore the possibilities to use generalized tools, such as FS for parameter scans of the GNM. FS calculates the BSM masses in the $\overline{\text{MS}}$ scheme at one loop “out of the box”. However, it does not neglect the off-diagonal terms, which are neglected as higher order contributions in Eq. (9). So far, we will use FS as a black box to get the pole masses of neutrinos and see if we get comparable results to the explicit calculations of Eqs. (9), (11), and (12).

4. Numerical comparison of pole masses

We compare the one-loop calculation and the FS calculation relative to the GL calculation. In order to do that, we do the following:

- From Eq. (11) and Eq. (12), we find a solution for d and d' that gives the experimentally measured mass differences [18] as pole masses, identifying

$$\mu_2^2 = \Delta m_{12}^2, \quad \mu_3^2 = \Delta m_{13}^2 \implies (d, d'). \quad (13)$$

- Instead of having a Yukawa coupling y , we parametrize it by the “mass correction” parameter Z_3

$$\frac{y^2 v^2}{2m_4} = m_3 = Z_3 \mu_3. \quad (14)$$

- The parameters d and d' are now functions of Z_3 , U_{PMNS} and the scalar potential parameters, *i.e.* of masses and mixings of the scalar particles, noted as m_S and U_S

$$(d, d')_i^{\text{GL}} = f_i(m_S, U_S, U_{\text{PMNS}}, \mu_4, Z_3). \quad (15)$$

- We take the benchmark point B1 from [19] for the scalar potential:

$$m_H = 300, \quad m_A = 411, \quad m_{H^\pm} = 442, \quad \text{GeV}, \quad \sin\theta_{H-h} \approx 0.07. \quad (16)$$

Then, the only free parameters are m_4 and Z_3 . We take the solutions for d and d' for given Z_3 and m_4 and put them as an input to FS and the $\overline{\text{MS}}$ renormalized expressions of Eq. (9), resulting in the mass values which we compare with the initial values of Eq. (13). We use `LoopTools` [16] to evaluate the expressions at the renormalization scale of 200 GeV, which is the scale at which FS does the pole mass calculation. In this way, we can compare the first order of the perturbation series: GL approximation *versus* one loop approximation *versus* FS pole mass calculation.

The numerical comparisons are presented in Fig. 3 and Fig. 4. To be sure that we do actually get the right solutions for d and d' , we check if we get the pole masses of Eq. (13) back. From Fig. 4, we can actually see that when

the heavy Majorana mass is higher than 10^6 GeV, we run into numerical problems in all of the calculations. In the range, where the calculation can be trusted, *i.e.* $m_4 < 10^6$ GeV, we see that the GL approximation (horizontal solid/orange line at zero) and one-loop approximation give quite different results in most of the ranges in Z_3 and m_4 . The FS calculation, in fact, is closer to the GL approximation. This hints the importance of the off diagonal terms even if they formally are of the higher loop order in the loop expansion. As the output of FS seems rather stable and not far from the GL approximation when the seesaw mass is less than 10^6 GeV, FS seems to be a promising tool to do parameter scans in this model.

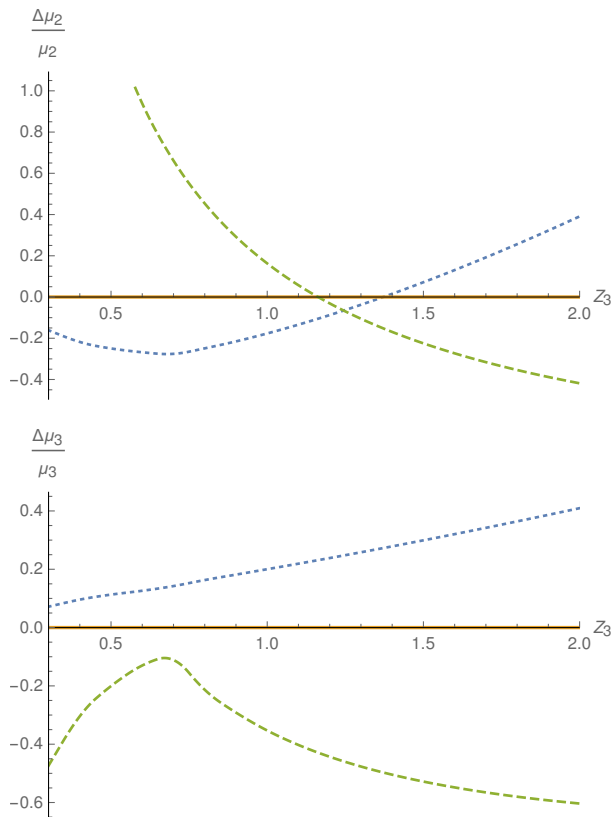


Fig. 3. (Color online) The difference between GL (solid, orange), one-loop (dashed, green) and FS (dotted, blue) pole mass calculations as functions of Z_3 with $m_4 = 10^5$ GeV, using the benchmark potential point from Eq. (16). The plot shows the relative differences of calculated pole masses *versus* pole masses in the GL approximation.

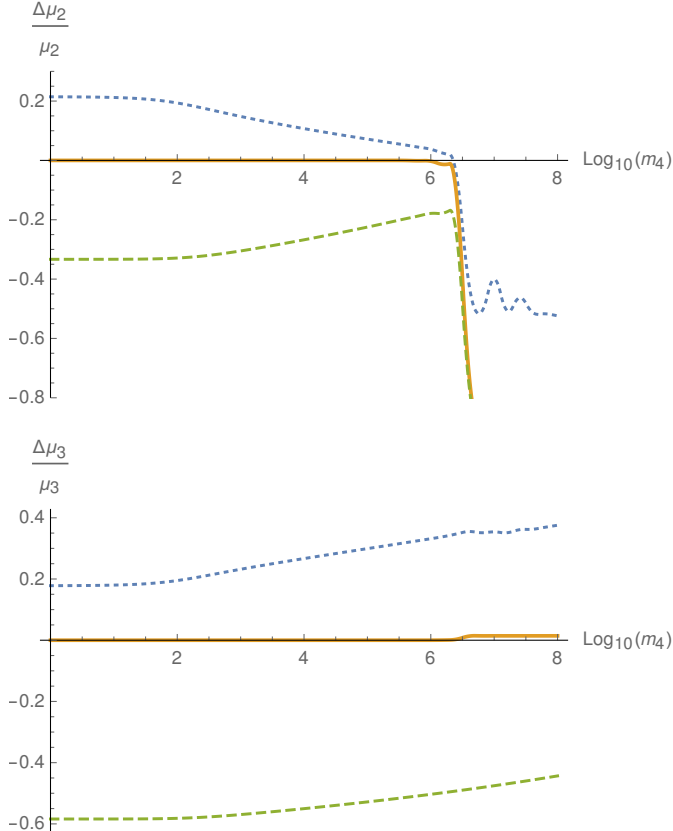


Fig. 4. (Color online) The difference between GL (solid, orange), one-loop (dashed, green) and FS (dotted, blue) pole mass calculations as functions of $\log_{10}m_4$ with $Z_3 = 1.5$, using the benchmark potential point from Eq. (16). The plot shows the relative differences of calculated pole masses *versus* pole masses in the GL approximation.

5. Conclusions

The seesaw mechanism has an interesting feature in perturbative pole mass calculations: the expansion in terms of couplings does not coincide with the expansion in terms of loops. When we expand in loops, the one-loop off-diagonal contributions to the mass matrix are neglected, since they are of a higher order in the perturbative expansion of the pole masses. By making an expansion in couplings, we could reproduce the expressions of the GL approximation [3]. We compared the pole mass calculations in these two expansions and found that they give significantly different results numerically. We also compared these calculations with the FS pole masses. The

FS results were closer to the GL approximation than our one-loop calculation. This could be explained by the importance of the off-diagonal terms in the GNM. To check if this is really the case, a calculation of pole masses with full one-loop 4×4 matrices will be done in the future and compared to the calculation of FS. So far, it seems that FS is a promising tool to do phenomenological studies with the GNM at least up to the seesaw scale of $\sim 10^6$ GeV, where numerical problems seem to go out of control.

The difference between one-loop calculations and GL calculations leads to an interesting question: when can we really trust a loop expansion and when the coupling expansion is more sensible? Since in some parameter cases the difference between the calculations could be as much as 50%, this looks like an important question to answer if we want to estimate the theoretical error of a calculation.

The authors thank the Lithuanian Academy of Sciences (the project DaFi2019) and the COST action CA16201 for funding. The authors thank Dominik Stöckinger and Wojciech Kotlarski for helpful discussions and Simona Draukšas for the initial FS file.

REFERENCES

- [1] P. Minkowski, *Phys. Lett. B* **67**, 421 (1977).
- [2] W. Grimus, H. Neufeld, *Nucl. Phys. B* **325**, 18 (1989).
- [3] W. Grimus, L. Lavoura, *Phys. Lett. B* **546**, 86 (2002).
- [4] W. Grimus, L. Lavoura, *J. High Energy Phys.* **0011**, 042 (2000).
- [5] P. Athron, J.-H. Park, D. Stöckinger, A. Voigt, *Comput. Phys. Commun.* **190**, 139 (2015).
- [6] P. Athron *et al.*, *Comput. Phys. Commun.* **230**, 145 (2018).
- [7] V. Dūdėnas, T. Gajdosik, *Phys. Rev. D* **98**, 035034 (2018).
- [8] D. Jurčiukonis, T. Gajdosik, A. Juodagalvis, [arXiv:1909.00752 \[hep-ph\]](https://arxiv.org/abs/1909.00752).
- [9] V. Dūdėnas, *Renormalization of Neutrino Masses in the Grimus–Neufeld Model*, Vilniaus Universiteto leidykla, 2019.
- [10] G.C. Branco *et al.*, *Phys. Rep.* **516**, 1 (2012).
- [11] E. Molinaro, *J. Phys.: Conf. Ser.* **447**, 012052 (2013).
- [12] H.K. Dreiner, H.E. Haber, S.P. Martin, *Phys. Rep.* **494**, 1 (2010).
- [13] V. Dūdėnas, <http://indico.if.us.edu.pl/event/5/contribution/46/material/slides/0.pdf>, 2019.
- [14] J.F. Donoghue, *Phys. Rev. D* **19**, 2772 (1979).
- [15] T. Hahn, *Comput. Phys. Commun.* **140**, 418 (2001).

- [16] T. Hahn, M. Pérez-Victoria, *Comput. Phys. Commun.* **118**, 153 (1999).
- [17] T. Hahn, S. Pašehr, C. Schappacher, *PoS LL2016*, 068 (2016) [*J. Phys.: Conf. Ser.* **762**, 012065 (2016)].
- [18] M. Tanabashi *et al.*, *Phys. Rev. D* **98**, 030001 (2018).
- [19] B. Hespel, D. López-Val, E. Vryonidou, *J. High Energy Phys.* **1409**, 124 (2014).